Journal of the Electrochemical Society

The Electrochemical Society
Advancing solid state & electrochemical science & technology

OPEN ACCESS

Quantification of Curcuminoids in Turmeric Using Visible Reflectance Spectra and a Decision-Tree Based Chemometric Approach

To cite this article: Hasika Suresh *et al* 2020 *J. Electrochem. Soc.* **167** 167528

View the article online for updates and enhancements.

Discover the EL-CELL potentiostats

- Fully independent test channels with Pstat / GStat / EIS
- Optionally with integrated temperature controlled cell chamber
- Unique Connection Matrix: Switch between full-cell and half-cell control at runtime

www.el-cell.com +49 (0) 40 79012 734 sales@el-cell.com

EL-CELL®
electrochemical test equipment

This content was downloaded from IP address 14.139.128.34 on 25/01/2021 at 09:12

Journal of The Electrochemical Society, 2021 **167** 167528

Quantification of Curcuminoids in Turmeric Using Visible Reflectance Spectra and a Decision-Tree Based Chemometric Approach

Hasika Suresh, Amruta Ranjan Behera,[z] Shankar Kumar Selvaraja, and Rudra Pratap

Center for Nanoscience and Engineering, Indian Institute of Science, Bangalore, India

For quantification of curcumin content in turmeric, a low-cost multivariate-analysis-based sensing system is desired. It can be realized by exploiting the spectra in the visible region, which enables the use of off-the-shelf, relatively inexpensive light sources and detectors. To address this, we propose a novel decision-tree method for improved prediction accuracy. Two sets of models with PLSR algorithm are developed with the measured reflectance spectra from 66 turmeric samples in the range of 360–750 nm, and their respective curcuminoids content are quantified by HPLC. A suite of a coarse-model for initial prediction of turmeric samples in the broad range of 1%–4%, and five finer-models for subsequent prediction (in the ranges 1%–2%, 2%–3%, 3%–4%, 1.5%–2.5%, and 2.5%–3.5%) constitute the proposed decision-tree approach. The method's efficacy is substantiated from an improved coefficient of determination (R^2) for the finer models (0.90–0.96) as compared to the coarse-model's 0.92. This is further corroborated with lower RMSECV of 0.06–0.13 and an RMSEP of 0.15–0.25 for finer models, as compared to 0.219 and 0.45 for the coarse model, respectively. Testing reveals that the method results in 46% reduction in prediction error. Realization of a robust prediction approach in the visible range sets the stage for the development of cost-effective field-deployable devices for on-site measurement of curcumin.

© 2021 The Author(s). Published on behalf of The Electrochemical Society by IOP Publishing Limited. This is an open access article distributed under the terms of the Creative Commons Attribution Non-Commercial No Derivatives 4.0 License (CC BY-NC-ND, http://creativecommons.org/licenses/by-nc-nd/4.0/), which permits non-commercial reuse, distribution, and reproduction in any medium, provided the original work is not changed in any way and is properly cited. For permission for commercial reuse, please email: permissions@ioppublishing.org. [DOI: 10.1149/1945-7111/abd603]

Manuscript submitted August 12, 2020; revised manuscript received November 30, 2020. Published January 4, 2021. *This paper is part of the JES Focus Issue on IMCS 2020.*

From modern literature to the books of traditional medicine, turmeric is hailed as one of the most important medicinal plants. Botanically, it belongs to the Zingiberaceae family. It is cultivated in the tropical and sub-tropical belts of the world, including India, Indonesia, South East Asia and Jamaica. As a food additive, turmeric imparts colour, flavor and also improves the shelf life of food products.[1] In the world of traditional remedies, it is used to alleviate a plethora of ailments including diabetic wounds, cough, joint pains, anorexia, etc.[2] The yellow bioactive compound in turmeric conferring these benefits, is Curcumin and it is known to show strong pharmacological activity as an anti-bacterial, anti-inflammatory and anti-cancerous[3,4] molecule. Structurally, it is a symmetrical molecule and has three chemical entities, two aromatic ring systems containing phenolic groups, connected by a seven-carbon linker. It has three forms based on the functional groups on the aromatic rings, called curcuminoids, namely curcumin, demethoxycurcumin and bisdemethoxycurcumin. Among these, curcumin is the largest contributor of the curcuminoids.

Quantifying these curcuminoids is essential for selecting the right variety of turmeric for any industry, that are till-date trying to explore all possible benefits this ancient spice has to offer. Among them, the nutraceutical industry that has a concomitant connection with turmeric, has made great advances in enhancing the bio-availability of curcumin through different nano-carriers and encapsulations of curcumin.[5] This, in turn, is helping the pharmaceutical industry that is trying to make intravenous injects of curcumin.[6] Monitoring the crucial steps through on going quantification of curcumin at every stage becomes of paramount importance. At the grass root level, the ability to quantify curcumin at the different stages of harvesting and post-harvesting will not only help in filtering the superior variety, but will also help the farmers get a better value for their crop.

A variety of analytical methods are used to analyse and quantify curcuminoids depending on the industrial need and quality obligations. The most popular ones are High Performance Liquid Chromatography (HPLC)[7] and its coupling to mass spectroscopy (LC-MS),[8] Thin Layer Chromatography (TLC),[9] supercritical extraction[10] and spectrophotometric techniques[11] as well as established techniques by ASTA.[12] These traditional laboratory methods have been used as the gold standard for quality control. However, such analyses are expensive and time consuming, requiring bulky instruments and usage of a plethora of chemicals, some even very toxic and hard to dispose. Industries that rely heavily on these tests for their manufacturing processes lose out on precious time while also adding to the woes of an already accumulating problem of waste management. A growing demand for faster, on-site quality analysis of food and agricultural produce with minimal sample preparation and chemical usage, has resulted in adoption of chemometric based techniques that have minimal or no sample preparation involved.

Fortunately, an upsurge in the use of spectroscopy as a non-destructive tool in both qualitative and quantitative analysis for a myriad of components is slowly gaining momentum. Spectroscopy combined with chemometrics is a powerful tool for determining physical properties and chemical signatures.[13,14] It has infiltrated into several fields including the food and beverage industry for classifying different food powders,[15] identifying adulterants,[16] monitoring fermentation of red wine,[17] tracking critical pharmaceutical steps,[18] and linking the evidence to the suspect in forensic sciences.[19] For our case in point, researchers have used various spectroscopic methods including diffused reflectance spectroscopy, Fourier Transform Infrared spectroscopy (FT-IR) and Raman spectroscopy, to predict the quantity of curcumin in turmeric samples.[20–22] Most of them, if not all, have exploited the NIR range (wavelength 700–2500 nm) to pick up signatures of specific chemical bonds in curcumin, and correlating the measured spectrum with the reference curcumin value. The reported accuracy for a predictive model has ranged between 91%–98%. Due to the recent developments in machine learning and cloud computing, there is a renewed interest from the spectrometer manufacturers to advance instrumentation with primary emphasis on miniaturization to exploit the IoT technologies. This had led to the development of several micro-spectrometers[15,23] with a parallel effort for their cost reduction. Since the cost for miniaturized light sources and detectors in the visible region is less than their NIR counterparts, our effort is directed towards enabling chemometric prediction of curcumin using the reflectance spectra in the visible range.

There are three critical aspects to a successful practical implementation of a chemometrics based system: presence of a spectral

[z]E-mail: amruta@iisc.ac.in

signature from the sample of interest, a reliable instrument for spectral acquisition, and a robust chemometric prediction model. We are focussing on the last part, as we see this as the missing element for curcumin estimation in turmeric. To the best of our knowledge, there are no reported chemometric models for estimation of curcumin in turmeric using the reflectance spectra in the visible range of the electromagnetic spectrum.

In this paper, we have explored curcumin's signature in the visible range (360–750 nm) and have used a decision-tree based chemometric approach through the construction of two kinds of models to predict curcumin, for improved accuracy. Affordable silicon detectors and availability of LED light sources in the sub-1000 nm and a set-up that can incorporate robust chemometric models can set the stage for the development of cost-effective field-deployable spectrometers for on-site measurements.

Materials and Methods

Sample collection and processing.—The sample-set for this study includes commercially procured turmeric powders as well as samples directly from farmers and traders. Dry turmeric roots were procured from different parts of India (Salem, Erode, Meghalaya and Kerala). The roots were first manually cut into small pieces (1 cm × 1 cm), followed by grinding them to a fine powder with a kitchen grinder. This powder was passed through a 250 μm industrial sieve to maintain uniform particle size. The turmeric powders were also hot air dried at 70 °C for four hours to remove the moisture from them. All analyses were performed on powders. The standard curcumin was purchased from SDFCL for HPLC analysis.

HPLC method for quantifying curcumin.—A turmeric sample/curcumin standard (95% pure) of 5 mg was accurately weighed and transferred to a 5 ml volumetric flask through a glass funnel. HPLC grade acetonitrile (SDFCL) was pipetted into the flask and filled up to the mark by the lower meniscus, making a stock concentration of 1 mg ml^{-1}. The flask capped with a glass screw was vortexed for 2 min at speed 6 (2500 rpm, -maximum speed) in a vortex mixer (IKA vortex Genius 3 mixer). One ml of this solution was centrifuged (Hermle-lav centrifuge) at 4000 rpm for 3 min to separate the supernatant and the undissolved particles. The supernatant was diluted with the mobile phase and injected into the HPLC. All samples were analyzed with HPLC (Agilent 1260 Infinity II with a quaternary pump and in an inbuilt degasser). A diode array detector (DAD) captured the spectral information at 425 nm. A stationary column of 4.6 mm × 50 mm and particle size of 2.7 μm (InfinityLab Porshell 120) were used for separating the mixture into its individual components. The temperature of the column was maintained at 40 °C. The mobile phase consisted of 0.2% ortho-phosphoric acid in de-ionized water and HPLC grade acetonitrile (55:45: v/v) used in isocratic mode throughout the 6 min run-time at a flow rate of 0.8 ml min^{-1}. The column was thoroughly purged with the mobile phase, ensuring a flat baseline before injecting any sample. The curcumin standard and the turmeric samples were run in triplicates. On separation, the individual peaks were identified and quantified by comparing the area under the curve of each turmeric sample against the area of the curcumin standard. The total curcuminoids are reported in g/100 g turmeric.

Spectra acquisition.—The spectra were acquired with JAZ spectrometer (from Oceanoptics, GMBH, Germany) in diffused reflectance mode and an external light source for increased probing intensity, and viewed in Ocean view (v. 1.6.7). The measurement set-up is depicted in Fig. 1. The range of measurement was from 360 nm to 1030 nm. For obtaining a smooth spectrum by reducing the noise associated with the measurement, some of the setting in the spectrometer were as follows: the averaging was set at 35 (number of scans internally taken to compute the mean spectrum), and boxcar-width (analogous to moving average) as 5. A single reflectance probe with two connectors (one for the light source and one for the spectrometer) was used for both illuminating the sample and collecting the reflected light from the sample. Integration time was set as per a white reference standard of barium sulphate, w.r.t. which, all the spectra were normalized after correcting for the dark spectra. The parameters that could potentially affect the reflected intensity from a sample were consistently maintained—the distance from the sample to the measuring probe, degree of compaction, and particle size distribution. Since the turmeric powder were already dried, variations in the scanned spectra due to the presence of moisture was minimized. With these measures in place, it is fair to assume that the sample-to-sample variations in reflected intensity represents the chemical distinctions to the best possible extent for each of the 15 scans taken per sample.

Data analysis.—The acquired spectra were analyzed with Unscrambler^{TM} software (v.11). Data sorting and arranging was done using Mathematica^{TM} (v.12) for easier and convenient importing. The samples were divided into training data ($n = 66$) and test data ($n = 10$). The correlation between the processed spectra and the curcumin content from HPLC analysis was examined by the partial least squared regression (PLSR) algorithm through the construction of two kinds of models (coarse and fine, as described later), for accurate prediction of curcumin content. The models were cross-validated on the test data sets. The model performance is reported with coefficient of determination (R^2) and root-mean-squared error of cross validation (RMSECV) and prediction (RMSEP) for the coarse and fine models.

Results and Discussion

Reference HPLC method.—Figure 2 shows the separation of the three curcuminoid fractions in the curcumin standard—95% (Fig. 2a) and a representative turmeric sample (Fig. 2b). As seen in the figure, there is good separation of each fraction in both the curcumin standard and the turmeric sample with the elution time being under 5 min. The retention time for Bisdemethoxycurcumin, Demethoxycurcumin and Curcumin were 2.937 ± 0.21, 3.365 ± 0.026, and 3.853 ± 0.032 min, respectively. For estimating the total curcumin content of each turmeric sample, the sum of all the three curcuminoids are considered.

Spectral analysis.—The spectra for all samples were recorded in diffused reflectance mode and converted to absorbance equivalents using Kubelka-Munk equation[24] for improved co-relation to the concentration of the analyte (as per Beer–Lambert's law). The spectra are recorded over the range of 360 nm–1030 nm. For this study, we have used the turmeric spectra in the visible range (360 nm–750 nm), as shown in Fig. 3a to build a regression model in order to quantify curcumin. The spectra of these 7 samples are a representative of all the samples in this data set. The spectra showed overlapping patterns beyond 750 nm and did not have any useful information to work with in this case. The visible spectrum of turmeric is mainly due to electronic transitions in bonding or lone-pair orbital and an unfilled non-bonding or anti-bonding orbitals.[25] The spectra have a broad peak between 400–500 nm, which is around the same wavelength range reported for liquid mode measurements of curcumin in solvents as well.[11]

The spectra from the instrument are often noisy, scattered, and sometimes might not show any visible peaks that can be used as features for the models in its raw form, as shown in Fig. 3a. Pre-processing steps enhance the data by correcting baseline offsets and surfacing hidden information through their derivatives. Here we describe the effect of each pre-processing steps applied to the data, in sequence.

- Multiplicative scatter correction (MSC)—MSC removes baseline shifts caused by both amplification (multiplicative) and off-set (additive) arising due to particle size or light scattering conditions. As seen in Fig. 3b, the MSC corrected spectra show a significant

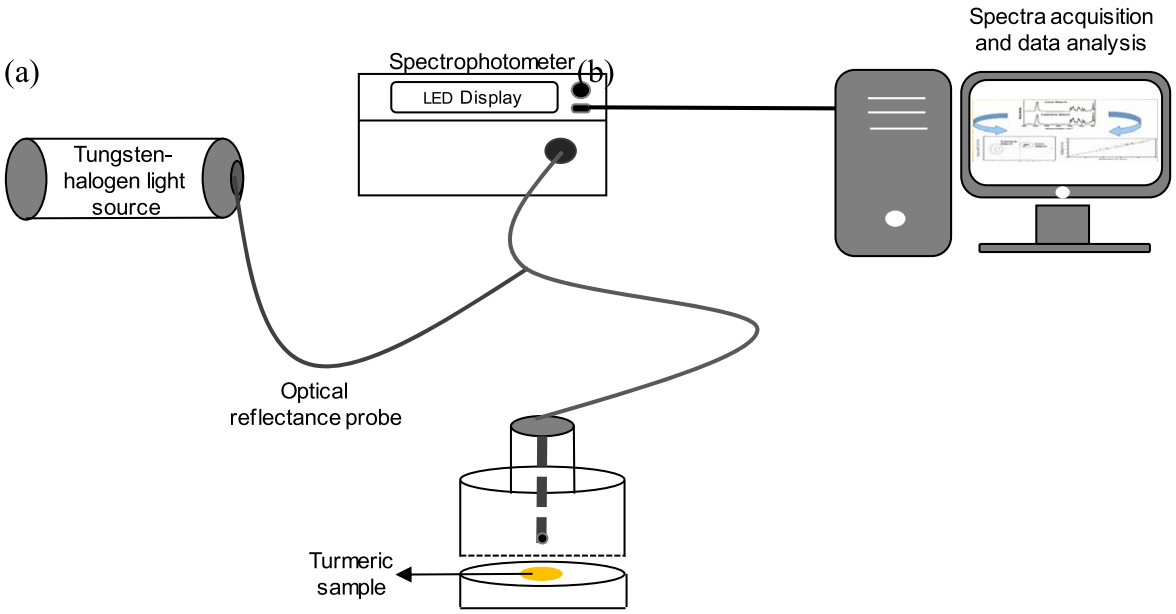

Figure 1. Measurement set up for spectra acquisition from powdered turmeric samples.

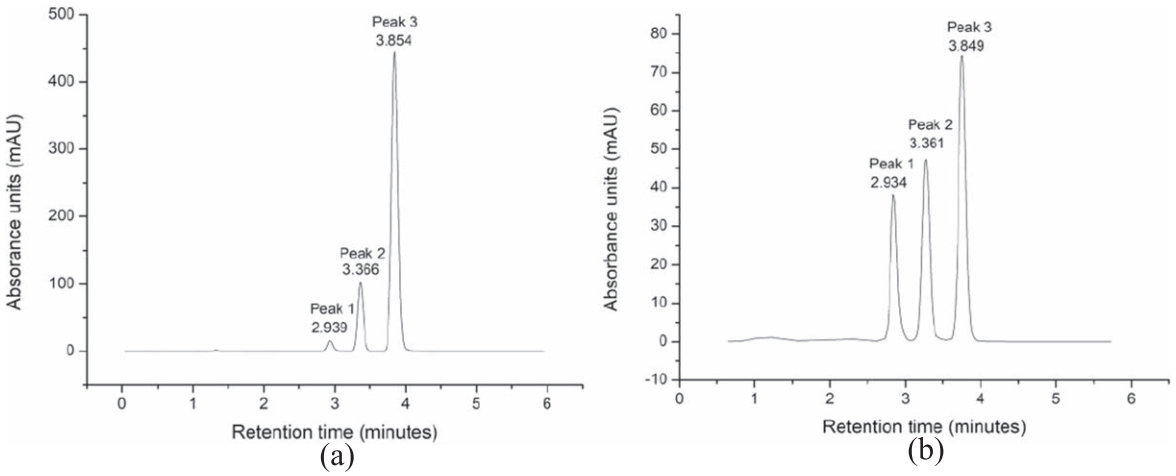

Figure 2. (a) HPLC chromatogram of standard curcumin (95%) showing three peaks representing the three fractions, namely, Bisdemethoxycurcumin (peak 1), Demethoxycurcumin (peak 2) and Curcumin (peak 3). (b) HPLC chromatogram of a representative turmeric sample.

reduction in scattering from 400–700 nm. The MSC method is believed to be the best suited for correction of spectra where the scatter variation is large in comparison to the chemical variation. In addition, the spectra should have relatively broad and strongly nonselective peaks.[26]

- Orthogonal scatter correction (OSC)—OSC minimizes the co-variance between X (wavelength) and Y (intensity) to maximize the orthogonality between X and Y.[27] As seen in Fig. 3c, OSC corrected data has features that are not present in the original spectrum, facilitating better interpretation of the models.
- Deresolve—A smoothening filter that allows to reduce the noise in the data (Fig. 3d).
- Savitzky-Golay filter—The application of the first derivative with Savitzky-Golay further highlights the spectral features as observed between 500–600 nm in Fig. 3e.

Decision-tree approach.—The curcumin value in turmeric varies from 1%–8% in dried fingers and bulbs and can go up to 10%–12% in mother samples.[28] To build a model to cater to the entire range requires extensive sample collection and a uniform spread of values over the entire range. For this study, we have undertaken to build a model for curcumin values ranging from 1%–4%, due to the predominant availability of samples in this range. The training model consists of 66 samples with 15 scans each (total—990 spectra), subjected to a combination of pre-processing steps of MSC, OSC, Deresolve and a Savitzky-Golay derivative filter (Fig. 3). For a qualitative data analysis, principal component analysis (PCA) is applied to the pre-processed data to visualize and remove evident outliers (Fig. 4). Each dot in the PCA scores plot represents the mean spectra of 15 scans per sample. The first two principal components explain 95% (PC1 + PC2) of the variation among the samples with respect to the wavelength range. There is subtle clustering when the spectra are divided into 1% curcumin slabs; indicating the similarities between those samples in terms of the principal components. The Hotelling's T^2 ellipse[29] is used to identify and remove outliers. Any point outside the ellipse is considered a potential outlier and can be removed to improve the model.

For quantitative data analysis, PLSR algorithm was used to construct a coarse model to quantify total curcuminoids in powdered turmeric samples using the HPLC data as the reference data. The model yielded a coefficient of determination (R^2) of 0.92 at PLS

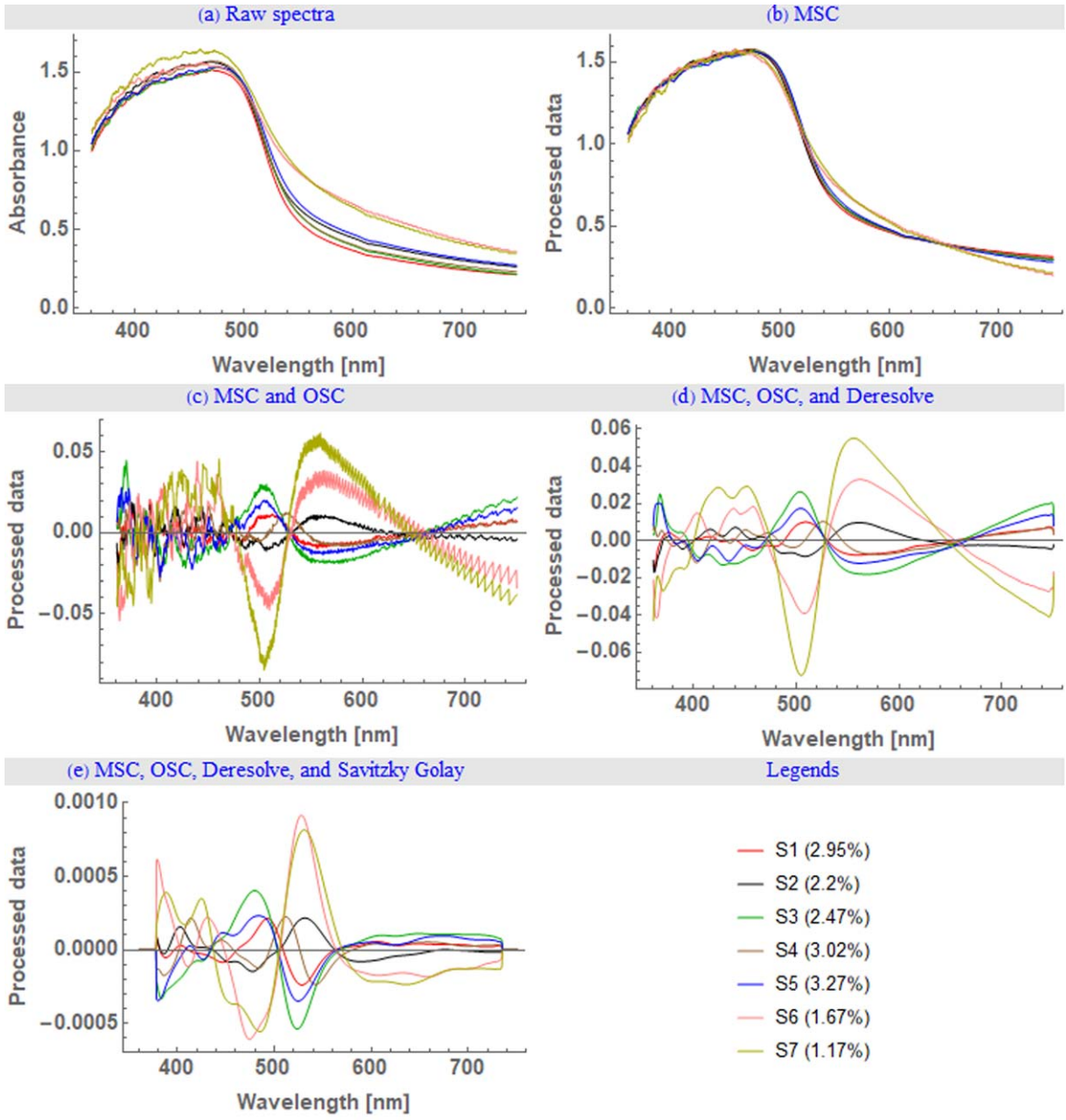

Figure 3. Images representing the transformation of the turmeric spectra when subjected to a sequence of pre-processing steps. (a) Raw turmeric spectra from the instrument. (b) MSC corrected spectra. (c) Spectra after applying OSC pre-treatment. (d) Application of Deresolve filter to smoothen the data (e) Spectra after the application of Savitzky-Golay filter.

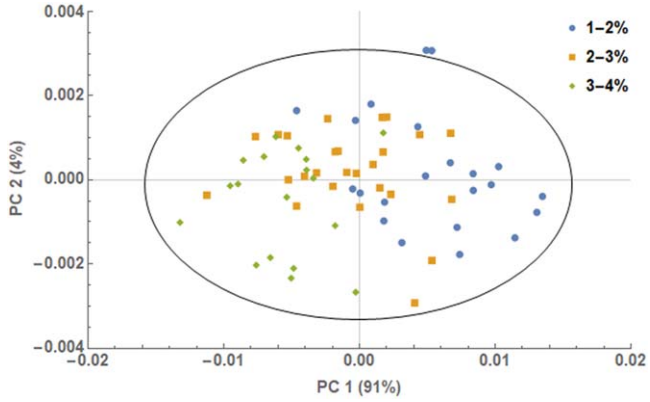

Figure 4. Scores corresponding to the first two principal components from the PCA along with the Hotelling's T^2 ellipse.

factor 7 with an RMSECV of 0.219 and an RMSEP of 0.45 on cross-validation with a test set of 29 samples, that were not a part of the training model. These samples had uniformly distributed curcumin values, over the 1%–4% range.

Owing to the diversity in the range of values and the need for poignant accuracy in quantifying the total curcuminoids through their spectrum, another set of models covering smaller curcumin ranges were constructed. The first set of fine models covered the range of 1%–2%, 2%–3% and 3%–4%, while the second set comprised models in the range of 1.5%–2.5% and 2.5%–3.5%. These two sets of models are depicted in Fig. 5. The numbers along the line designate the percentage curcumin content. The first and second set of fine models are represented by the green bands above and below the line, respectively. The second set of models are offset by d (=0.5%) w.r.t. the first set, where d is half of a model's span (=1%), to deal with boundary cases as will be described below. Once the initial prediction from the coarse model is obtained along with the error ($Y \pm \Delta Y$), the decision rules for choosing the

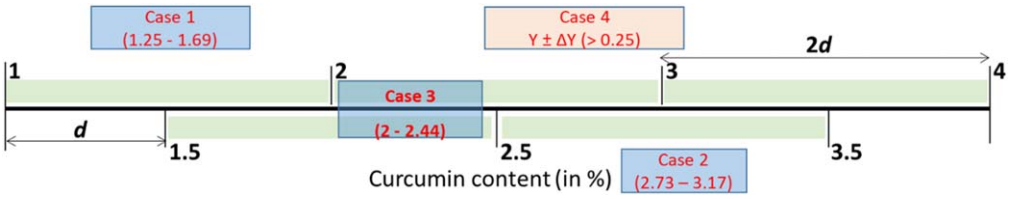

Figure 5. Representation of the decision- tree approach for selection of the suitable fine.

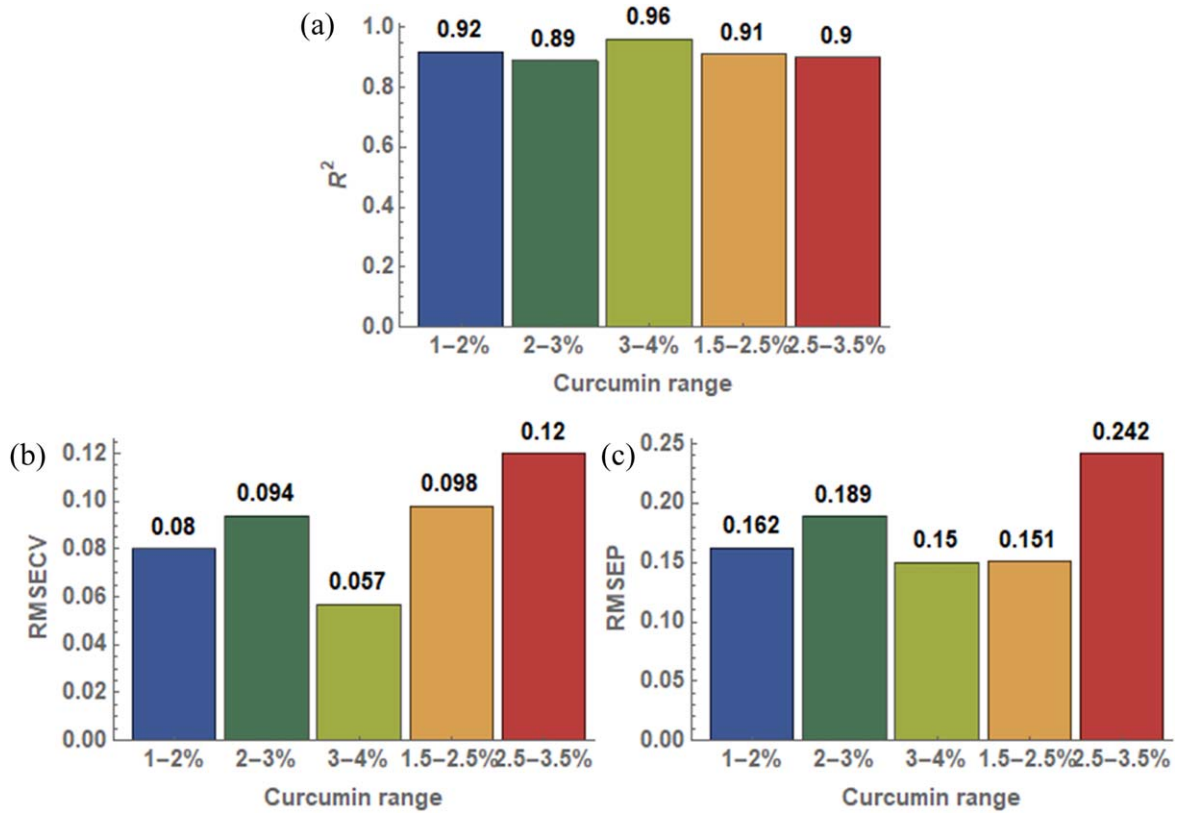

Figure 6. Bar charts illustrating model parameters for each of the fine models: (a) Coefficient of determination (R^2), (b) Root-mean-squared error of cross-validation (RMSECV), (c) Root-mean-squared error of prediction (RMSEP).

appropriate fine model for final assessment based on the predicted range (Y-ΔY, Y+ΔY), are as follows:

If the range completely fits within the scope of one fine model, then that model is chosen. Two such example cases are described here: (*i*) Case 1: The range predicted by the coarse model is 1.25%–1.69% (sample 10), which implies that the appropriate fine model is 1%–2%. (*ii*) Case 2: The range predicted by the coarse model is 2.73%–3.17% (sample 8), therefore, the appropriate fine model is 2.5%–3.5%, and not 2%–3% or 3%–4%. If the range completely fits within the scope of two fine models, then the average of both model's prediction is used. An example is sample 3 (case 3), for which the coarse-model-predicted range is 2%–2.44%. Both fine models 2%–3% and 1.5%–2.5% should be used for prediction and their average value should be considered as the final value.

These conditional steps form the basis of the proposed decision-tree approach. It must be noted here that there is a relation between the acceptable error for the coarse model (ΔY) and the staggered offset (d) between the boundaries of two sets of fine models. For the logical approach described in the above three cases, it is assumed that the coarse model error (ΔY) is less than 0.25, which is the case in this study ($\Delta Y = 0.219$). However, if the error is larger than 0.25, then an ambiguous situation may arise (shown as case 4) when the range overlaps into the scope of 4 finer models. The present set of finer models is not suitable for such scenarios. Thus, it leads to defining a rule-of-thumb of $2\Delta Y < d$ for specifying the boundaries of fine models in a decision-tree approach like the one proposed here.

Each of these finer models were also subjected to a combination of four pre-processing steps, i.e., OSC, MSC, Deresolve, and Savitzky-Golay first derivative, with the exception for the curcumin range 3%–4%, where OSC was not used, as this sample set did not need an additional feature extraction step. The coefficient of determination (R^2) and RMSECV for each of the fine models constructed with the PLSR algorithm is reported in Fig. 6. The two model parameters, R^2 ranged from 0.90 to 0.96 (Fig. 6a) and the RMSECV varied from 0.06 to 0.13 (Fig. 6b), showing better performance than the corase model. Each of the fine models was also cross validated with a test data set and the RMSEP was in the range of 0.15–0.25 (Fig. 6c).

Ten samples out of the 29 test samples were chosen to demonstrate this approach. The results from all the steps of the decision-tree approach are summarized in Table I, along with the final predicted value of curcumin from the inferred fine model. Figure 7 shows the diagrammatic representation of the final validation results for test samples that were not included in the

Table I. Results from the decision-tree approach followed to choose the suitable fine model for 10 test samples, and the final prediction of curcumin content.

Sample ID	Actual curcumin content (x %)	Coarse model predicted value (y %)	y -0.219	$y + 0.219$	Inferred fine model	Final predicted value of curcumin (z %)
1	2.75	2.82	2.60	3.04	2.5%–3.5%	2.7
2	2.21	1.90	1.68	2.12	1.5%–2.5%	2.03
3	2.13	2.22	2.00	2.44	2%–3%	2.15
4	2.19	2.47	2.25	2.68	2%–3%	2.4
5	2.75	2.85	2.63	3.07	2.5%–3.5%	2.83
6	3.64	3.92	3.70	4.14	3%–4%	3.8
7	3.02	2.76	2.54	2.98	2.5%–3.5%	3.04
8	3.27	2.95	2.73	3.17	2.5%–3.5%	3.24
9	1.76	1.27	1.05	1.49	1%–2%	1.31
10	1.24	1.47	1.25	1.69	1%–2%	1.39

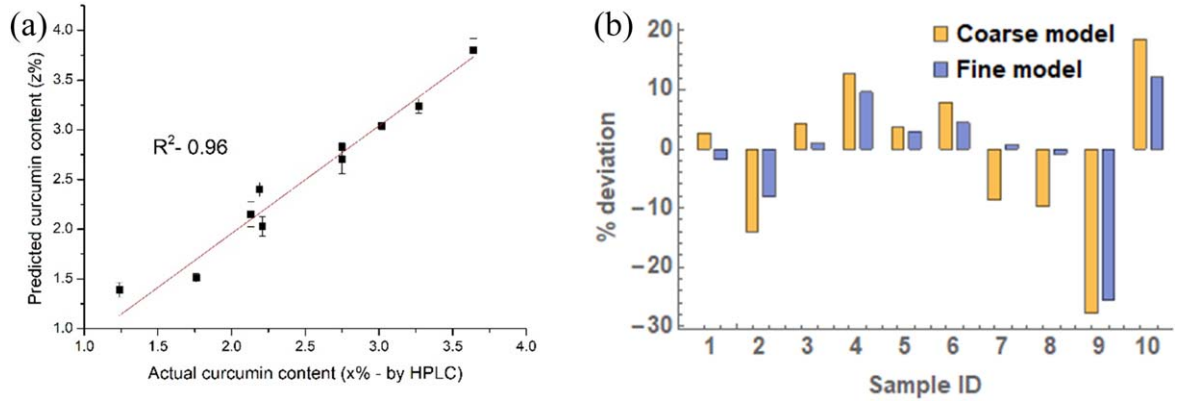

Figure 7. (a) Scatter plot showing the final predicted value of curcumin vs the actual curcumin content from HPLC. (b) Deviation plot for predicted values from the coarse model and their respective inferred fine model.

calibration model. The higher the coefficient of determination (R^2), the better the correlation between the actual curcumin value and the predicted value (quantities x and z from Table I, respectively). These values are depicted in Fig. 7a and R^2 was found to be 0.96. The points correspond to the mean, and the error-bars represent the variations among the predicted curcumin values corresponding to the 15 scans of a particular sample. Based on the mean and the standard-deviation of the 15 predicted values for a sample, the variation was found to be in the range of 1%–5%, which shows reasonable repeatability. To further strengthen our claim of improved accuracy with the decision tree approach, the deviations in both the predicted values from the coarse model(y) and from the inferred fine model(z), w.r.t. the actual values(x) were analyzed. As seen in Fig. 7b, there is an evident decrease in the deviation in the fine model predictions as compared to the coarse model, for all the 10 samples, which indicates closer prediction to the actual value of curcumin content in these turmeric samples. The prediction errors from a fine model for 10 samples was found to be 46% less as compared to the coarse model prediction errors.

Conclusions

This study shows that visible spectroscopy coupled with chemometrics can be used as a non-destructive tool to quantify total curcuminoids in a diverse variety of powdered turmeric samples. The samples used here represent the most prevalent varieties with 1%–4% curcumin content. A decision-tree approach for improved accuracy is also established through the construction of a coarse and fine model for curcumin prediction, which is shown to result in an average of 46% reduction in the prediction error. The coefficient of determination for the validation set was 0.96, showing a strong correlation. The repeatability error for prediction was within 5%. Realization of a robust prediction approach in the visible range sets the stage for the development of cost-effective field-deployable devices for on-site measurement of curcumin in turmeric samples.

Acknowledgments

This work is primarily catalyzed and supported by the Office of the Principal Scientific Adviser to the Government of India and partially by a grant from the Government of Karnataka.

ORCID

Amruta Ranjan Behera https://orcid.org/0000-0002-0972-3120
Shankar Kumar Selvaraja https://orcid.org/0000-0003-2670-7058

References

1. R. K. Maheshwari, A. K. Singh, J. Gaddipati, and R. C. Srimal, *Life Sci.*, **78**, 2081 (2006).
2. I. Chattopadhyay, K. Biswas, U. Bandyopadhyay, and R. K. Banerjee, *Turmeric and Curcumin: Biological Actions and Medicinal Applications*, **87**, 44 (2004), https://www.jstor.org/stable/24107978.
3. H. Ahsan, N. Parveen, N. U. Khan, and S. M. Hadi, *Chem. Biol. Interact.*, **121**, 161 (1999).
4. M. Kaur, A. Singh, B. Kumar, S. K. Singh, A. Bhatia, M. Gulati, T. Prakash, P. Bawa, and A. H. Malik, *Eur. J. Pharmacol.*, **805**, 58 (2017).
5. Z. Rafiee, M. Nejatian, M. Daeihamed, and S. M. Jafari, *Crit. Rev. Food Sci. Nutr.*, **59**, 3468 (2019).
6. Y. Gao, Z. Li, M. Sun, C. Guo, A. Yu, Y. Xi, J. Cui, H. Lou, and G. Zhai, *Drug Deliv.*, **18**, 131 (2011).
7. W. Wichitnithad, N. Jongaroonngamsang, S. Pummangura, and P. Rojsitthisak, *Phytochem. Anal.*, **20**, 314 (2009).
8. R. Hiserodt, T. G. Hartman, C. T. Ho, and R. T. Rosen, *J. Chromatogr. A*, **740**, 51 (1996).
9. P. Phattanawasin, U. Sotanaphun, and L. Sriphong, *Chromatographia*, **69**, 397 (2009).
10. B. Gopalan, M. Goto, A. Kodama, and T. Hirose, *J. Agric. Food Chem.*, **48**, 2189 (2000).
11. K. Sharma, S. S. Agrawal, and M. Gupta, *Int. J. Drug Dev. & Res.*, **4**, 375 (2012), https://www.researchgate.net/publication/285665708.
12. *Official Analytical Methods of the American Spice Trade Association* (Method 18.0, Englewood Cliffs, NJ) 4th ed. (1997).
13. P. Geladi and E. Dåbakk, *J. Near Infrared Spectrosc.*, **3**, 119 (1995).
14. K. Héberger, *Med. Appl. Mass Spectrom.*, 141 (2008).
15. H. You, Y. Kim, J. H. Lee, and S. Choi, *Int. Conf. Ubiquitous Futur. Networks, ICUFN*, 732 (2017).
16. S. Medina, R. Perestrelo, P. Silva, J. A. M. Pereira, and J. S. Câmara, *Trends Food Sci. Technol.*, **85**, 163 (2019).
17. D. Cozzolino, M. Parker, R. G. Dambergs, M. Herderich, and M. Gishen, *Biotechnol. Bioeng.*, **95**, 1101 (2006).
18. J. Rantanen, H. Wikström, R. Turner, and L. S. Taylor, *Anal. Chem.*, **77**, 556 (2005).
19. R. Chophi, S. Sharma, and R. Singh, *Forensic Chem.*, **17**, 100209 (2020).
20. Y. J. Kim, H. J. Lee, H. S. Shin, and Y. Shin, *Phytochem. Anal.*, **25**, 445 (2014).
21. K. Thangavel and K. Dhivya, *Eng. Agric. Environ. Food*, **12**, 264 (2019).
22. I. M. A. G. Wirasuta, C. I. T. R. Dewi, N. P. L. Laksmiani, I. G. A. M. Srinadi, and D. P. Putra, *Indones. J. Pharm. Sci. Technol.*, **5**, 88 (2018).
23. J. T. Daly, E. A. Johnson, W. A. Bodkin, W. A. Stevenson, and D. A. White, *Silicon-based Optoelectronics II*, ed. D. J. Robbins and D. C. Houghton (SPIE) 3953, p. 70 (2000).
24. A. A. Christy, O. M. Kvalheim, and R. A. Velapoldi, *Vib. Spectrosc.*, **9**, 19 (1995).
25. H. Van Nong et al., *Springerplus*, **5**, 1147 (2016), [http://springerplus.springeropen.com/articles/10.1186/s40064-016-2812-2].
26. T. Isaksson and B. Kowalski, *Appl. Spectrosc.*, **47**, 702 (1993), [http://journals.sagepub.com/doi/10.1366/0003702934066839].
27. J. Trygg and S. Wold, *J. Chemom.* (Wiley, New York) 17, p. 53 (2003), [https://onlinelibrary.wiley.com/doi/full/10.1002/cem.775].
28. H. H. Tønnesen, J. Karlsen, S. R. Adhikary, and R. Pandey, *Z. Lebensm. Unters. Forsch.*, **189**, 116 (1989).
29. J. E. Jackson, *A Use's Guide to Principal Components* (John Wiley & Sons, United States of America) (1991).